

Hydrogen generation over $\text{TiO}_2 - \text{Al}_2\text{O}_3 - \text{Rh}$ catalyst by partial oxidation of propane

V.Subramanian^{1*}, J. Choi,² R.Z. Ni³, E.G. Seebauer³, R.I. Masel³

¹University of Nevada, Department of Chemical and Metallurgical Engineering
Tel: 775-784-4686, Fax: 775 327 5059, email: ravisv@unr.edu
Room 310/ LMR 474/ Mail stop 388, Reno, NV, 89557 – 0030

²POSTECH, Department of Chemical Engineering, South Korea

³University of Illinois, Department of Chemical and Biomolecular Engineering
Roger Adams Lab, 600 South Mathews, Urbana, IL 61801

Abstract

This article presents the development and application of $\text{TiO}_2 - \text{Al}_2\text{O}_3$ as supports for propane to hydrogen conversion. Phase transformation of oxide supports during high temperature processes ($>500^\circ\text{C}$) can cause their surface area to decrease. In the first part of this communication, synthesis and characterization of a thermally stable $\text{TiO}_2 - \text{Al}_2\text{O}_3$ mixed oxide support is presented. This composite oxide demonstrates no phase transformation (anatase \rightarrow rutile), maintains surface area even after heating to 900°C , and continues to do so following several heat and cool cycles. Further, we demonstrate that the $\text{TiO}_2 - \text{Al}_2\text{O}_3$ support improves hydrogen yield from propane partial oxidation by 30% compared to using Al_2O_3 alone as the support. An optimal hydrogen yield is obtained with a $\text{TiO}_2 - \text{Al}_2\text{O}_3$ composite of 0.54:0.46 weight ratio deposited with Rhodium operating at 900°C . Long-term operation shows that TiO_2 delays catalyst deactivation, but only up to 25 hours.

Keywords: partial oxidation, $\text{TiO}_2 - \text{Al}_2\text{O}_3$, rhodium, propane, hydrogen

1 - INTRODUCTION

Hydrogen production has been the focus of much research as a possible efficient and alternative fuel source [1, 2]. Hydrogen can be used to power devices over a range from mW (portable systems) to kW (on site power generation). High temperature reforming over catalysts supported on oxides is an effective method for producing hydrogen. In a portable application, power generation can involve the use of a microdevice (microreformer) to produce hydrogen. The advantages of a microdevice includes high hydrocarbon to hydrogen conversion efficiency due to large surface to volume ratio of the support. However these devices are subject to thermal shocks during startup and shut down. High operating temperatures $>600^\circ\text{C}$ result in catalyst deactivation by sintering and thermal shocks lead to oxide support aggregation.[3-5] Both these limitations are particularly difficult to prevent. An ideal support is one that would undergo minimal aggregation due to thermal shocks and maintain its surface area over a wide range of temperatures. One promising approach is to prepare a support consisting of composite materials that incorporate the beneficial aspects of the added constituents.[6]

Propane is the focus of this study because it has a high energy density (7.5KWh/l), produces more hydrogen per unit weight (compared to for example methanol[7]), is widely available, and easily transported through existing infrastructures. A few reports discuss the application of mixed oxides as supports for catalytic conversion of propane (oxidation [8], dehydrogenation.[9]) It has been shown that the optimal temperature for propane partial oxidation (POx) is

$>900^\circ\text{C}$. [10] So far, propane POx to produce hydrogen has been performed over oxides such as Al_2O_3 . [7,10-13] Further, it has been found that the presence of TiO_2 favors particularly low CO generation [14] and higher selectivity toward hydrogen.[15] TiO_2 also promotes catalytic activity due to high surface area at low temperatures but suffers from poor thermal stability due to phase transformation; Al_2O_3 has high stability at low temperatures.[16] However no long term performance results were known with these supports. Besides, the effects of thermal shocks (startup/shutdown) on the support-catalyst composites had not been well understood.[17] Therefore, our objective is to synthesize a $\text{TiO}_2 - \text{Al}_2\text{O}_3$ mixed oxide composite that offers higher thermal stability and improved hydrogen yield.

2 - EXPERIMENTAL SECTION

2.1 - Chemicals

Titanium butoxide (Aldrich, $>99\%$), glacial acetic acid, 2-propanol, and deionized water were used for the synthesis of TiO_2 colloids. The butoxide precursor was employed because Bacsa has reported minimal rutile formation with this precursor.[18] Al_2O_3 (obtained from Degussa®) was used without further treatment. The data provided by Degussa are as follows: specific surface area, $100 \pm 15 \text{ m}^2/\text{g}$; average primary particle size is 13 nm; Al_2O_3 content, $\geq 99.6 \text{ wt } \%$. Phase details were obtained by X-ray powder diffraction (XRPD) as will be discussed later. The sol-gel synthesis technique was adapted to prepare colloidal TiO_2 . Rhodium chloride was obtained from Aldrich Chemical Company.

2.2 - Synthesis methods

The sol-gel synthesis technique was adapted to prepare colloidal TiO_2 . Details of the procedure are available in a recently published article.[19] After the colloids were prepared, the solution remained stable for many days. To prepare a composite oxide, known amounts of Al_2O_3 powder was added to the TiO_2 sol on a weight basis. A step-by-step heating protocol to from room temperature to 900°C was employed to transform the phase of the composite. The first began with heating from 25°C to 130°C over 1 h. This was followed by heating from 130°C to 900°C over 6 h. the oxide was then maintained at a constant temperature of 900°C for 6 h. The resulting material was subsequently cooled from 900°C to 25°C gradually over 6 h by convection in air. For depositing Rhodium, a $\sim 10\text{ml}$ solution of rhodium chloride in water (1mg Rh salt/1ml of water) was prepared. 0.3ml of this salt solution was added drop wise to 0.8g of mixed oxide powder. Deionized water (2ml) was added, and the mixture was sonicated to ensure homogeneous wet impregnation. Excess water was evaporated by slow drying at $\sim 80^\circ\text{C}$ overnight. Reduction of the Rhodium was performed by loading the oxide – Rhodium mixture onto a quartz tube at 600°C for 2hr in a 100 sccm flow of 8.5% Hydrogen – 91.5% Helium.

Propane, oxygen, and nitrogen were obtained from S. J. Smith®. A customized quartz tube with a ceramic frit was used as the test reactor for propane POx. All experiments were performed with 0.8 g of oxide support. Metal loading was maintained at 3.5 ± 0.02 wt%. The reacted gas mixture was collected in a gas-sampling chamber, and the contents were analyzed with an SRI® 8610C gas chromatograph. The feed gas consisted of a mixture of propane, oxygen, nitrogen, and helium with the following ratio: 10:19:5:271 (in sccm controlled by an MKS® regulator). Nitrogen was used as an internal standard for calibration. The temperature was varied between 500°C and 900°C in a Lindberg®/Blue tube furnace. Each reaction was run for 0.5 h prior to sampling to ensure steady state. The samples were injected in a 100/120 20ft Hayesep D Restek® column. Helium was used as the carrier gas at a flowrate of 40 ml/min. The oven of the gas chromatograph was operated at 40°C for the first 5 minutes, followed by ramping up to 200°C at $6^\circ\text{C}/\text{min}$.

2.3 - Characterization techniques

The Brunauer-Emmett-Teller (BET) method was used to estimate the oxide support surface area. Nitrogen was used as the probe gas with a Micromeritics Ltd [Pulsed Chemisorb (Chemisorb) model no. 2705] multipurpose instrument. The same instrument was also used to measure the dispersion of Rhodium on the mixed oxide with hydrogen chemisorption. The oxide composites were also characterized using a general-area detector diffraction system (GADDS-Bruker) system to measure the X-ray powder diffraction (XRPD) pattern. The particle size was estimated using the Scherrer equation ($t=C\lambda/B\cos\theta$, where where $C = 0.9$, λ is the X-ray wavelength, B is the full width at half-maximum corrected for

instrumental broadening, and θ is measured Bragg angle). A standard lanthanum hexafluoride sample from NIST was used to account for instrumental broadening.

3 - RESULTS AND DISCUSSIONS

3.1 - XRPD of the $\text{TiO}_2 - \text{Al}_2\text{O}_3$ powder

The XRD of the oxide composite was performed over a range of $2\theta = 20-65^\circ$ in a split pattern ($2\theta = 20-45^\circ$ and $40-65^\circ$). While peaks corresponding to both TiO_2 and Al_2O_3 could be observed for the mixed oxides, no peaks indicating formation of any Ti-Al compounds were detected. TiO_2 typically undergoes the following sequence of phase transformation: amorphous-anatase-brookite-rutile.[20-22] when heated to high temperatures. The formation of brookite phase is believed to accelerate the anatase to thermodynamically more stable rutile phase causing surface area to decrease. [20, 21] Therefore, from a stability point of view, our interest was to

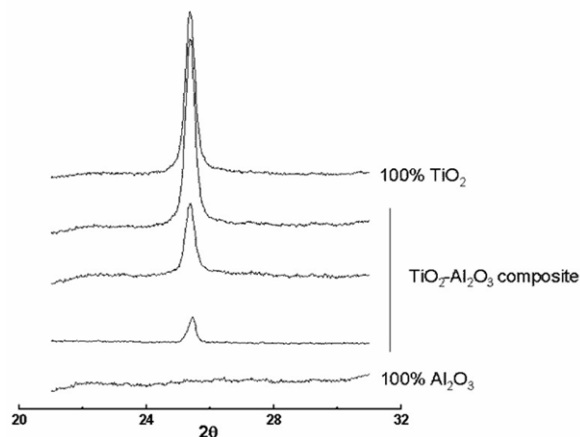


Figure 1 Slow – scan XRPD pattern of the mixed oxide with different compositions From bottom to top: Ti(0), Ti(0.25), Ti(0.43), Ti(0.64), and Ti(1). The only peak observed in the figure corresponds to anatase phase of TiO_2 .

find out if the brookite phase was present. Slow scan XRPD was performed to answer this question. Figure 1 shows the slow scan data for oxides over $21 - 32^\circ$ at $0.15^\circ/\text{min}$ (a region where brookite, if present, would be detected) for different composite ratios. No brookite phase was identified. In general, although addition of Al_2O_3 to the TiO_2 sol facilitates the delay of TiO_2 phase transformation from anatase to rutile, we did not notice any phase transformation of even pure TiO_2 . This indicates that TiO_2 can exist in anatase phase independently even after calcination at 900°C . The alumina phase was identified as that corresponding to the delta phase (ICSD No. 82604) while the TiO_2 phase was found to be anatase (ICSD No. 96946).

3.2 - Oxide support stability

Further analysis to evaluate the stability of the mixed oxide was performed by subjecting the oxides to heat and cool cycles between the temperature ranges of 25°C to 900°C . The

surface area of the oxides was measured after each of this heat-cool cycle. The changes in the surface area are plotted as a function of the cycle number in Fig. 2. From the figure it is noted that all mixed oxides loose ~15% of their initial surface area within the first 2-3 heating cycles. Any further heating does not cause the surface area to decrease. We performed the cycle 4 additional times and found the surface area to be

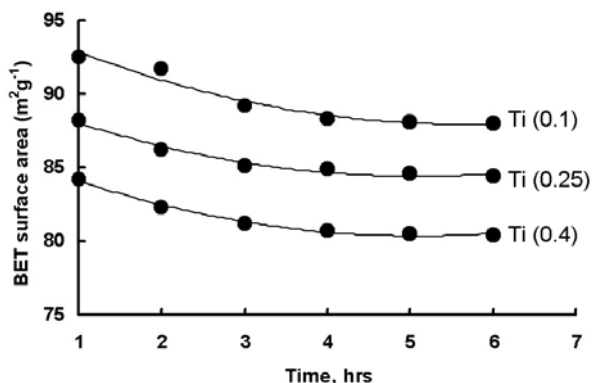


Figure 2 This figure shows the surface area of the mixed oxide after calcination at 900°C. The surface area of the oxide is stable following several heat – cool cycles.

stable. This shows that the oxide is stable under thermal shocks and could be used as a support for microreformers. Phase transformation in a material is dictated by the thermodynamic driver to achieve lowest possible surface energy/unit volume.[23, 24] According to this concept, as the particle size decreases, grain growth rates increases.[21] This leads to an acceleration in grain boundary growth which results in the development of irregularities in the form of crystal twinning planes.[25] The defects offer sites for nucleation of brookite phase that triggers rapid phase transformation from anatase to rutile. [20, 22] Our experiments did not show any brookite phase even with very slow scan rates. The absence of rutile phase can thus be attributed to the absence of brookite phase formation after calcination.

3.3 - Chemisorption

The extent of metal dispersion was determined by hydrogen chemisorption over Rhodium at 35°C. The dispersion of the metal was almost doubled in the presence of TiO₂. In a related study, higher dispersion of Palladium were reported in an in the presence of TiO₂. [26] Particle sizes of Rhodium were 11±3 nm and 8±2 nm over Al₂O₃ and TiO₂ – Al₂O₃ after reduction. This result shows that the presence of TiO₂ as a component of the mixed oxide with Al₂O₃ promotes formation of smaller and hence more dispersed Rhodium.

3.4 - Propane partial oxidation

Figure 3 shows the hydrogen yield over Al₂O₃ and TiO₂ – Al₂O₃. We observed that the hydrogen yield improves when TiO₂ is present. As the concentration of TiO₂ increases up to 54 wt %, the hydrogen yield increases. Above this TiO₂

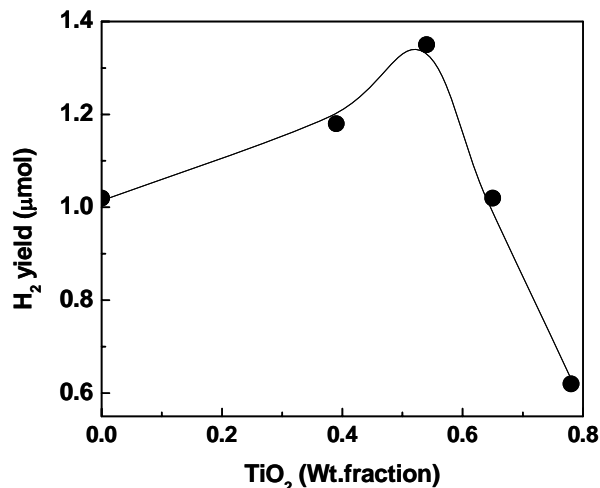


Figure 3 This figure shows the Hydrogen yield from propane partial oxidation over TiO₂-Al₂O₃ of different weight ratios. Operating conditions: Rh – 3.5±0.02wt %, flowrate 305 sccm.

loading, the hydrogen yield decreases rapidly, and becomes to less than that of Al₂O₃ alone above 65 wt %. At the optimum composition of 54 wt % TiO₂, 30% improvement in hydrogen yield is possible. While this result was for 0.8g of the total mixed oxide support weight, similar results of higher hydrogen yield at 54wt% TiO₂ were obtained at different total weights of TiO₂-Al₂O₃ loading compared to Al₂O₃.

3.5 - Effect of long term operation

For commercial applications, it is essential that catalyst and catalyst supports maintain reasonable operation over 100s of hours. [27] Further, complete conversion of propane usually occurs at high temperatures (>750°C). [10, 28, 29] The goal here was to examine the activity of the catalyst–support complex to achieve propane to hydrogen conversion at the

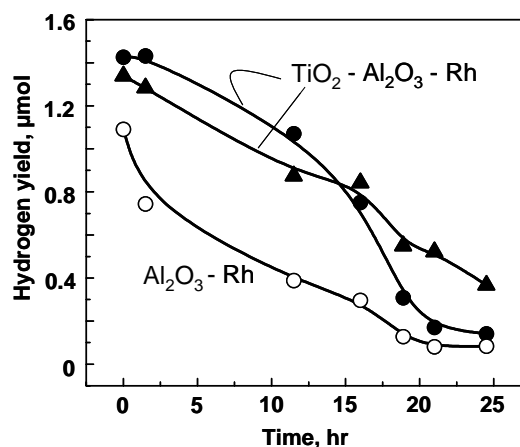


Figure 4 Hydrogen yield from propane partial oxidation over (a) Al₂O₃, (b) TiO₂ – Al₂O₃ (TiO₂ wt.% 54), and (c) TiO₂ – Al₂O₃ (TiO₂ wt.% 40)

highest possible temperature, i.e. 900°C for as long as

possible. We observed maximum hydrogen yield at 900°C for a TiO₂-Al₂O₃ composite with 54 wt% TiO₂. (results not shown). These experiments were performed after a steady state reaction time of 30 minutes. Often, longer-term catalyst operation can lead to a decrease in catalytic activity. To investigate this possibility, hydrogen generation was monitored at 900°C over 25 hours of operation for the TiO₂-Al₂O₃ composite. Figure 4 shows these results along with the hydrogen yield over Al₂O₃. The hydrogen yield decreases by 70% in 12 hr over Al₂O₃. By contrast, the yield over 54 wt% TiO₂ shows a decrease of only 35% over the same period. Similar results were also observed over TiO₂ 40wt %. However, at the end of 25 hr, the hydrogen yield over both materials continues to decrease in such a way that the yield for TiO₂-Al₂O₃ is almost similar to the yield over Al₂O₃.

ACKNOWLEDGEMENTS

This work was supported by the Department of Defense Multidisciplinary University Research Initiative (MURI) program administered by the Army Research Office under Contract DAAD19-01-1-0582.

REFERENCES

- [1] Dicks, A. L., "Hydrogen generation from natural gas for the fuel cell systems of tomorrow," *J Power Sources*, vol. 61, pp. 113-124, 1996.
- [2] Koroneos, C., Dompros, A., Roubas, G., and Moussiopoulos, N., "Life cycle assessment of hydrogen fuel production processes," *Int J Hydrogen Energ*, vol. 29, pp. 1443-1450, 2004.
- [3] Forzatti, P. and Lietti, L., "Catalyst deactivation," *Catal Today*, vol. 52, pp. 165-181, 1999.
- [4] McCarty, J. G., Gusman, M., Lowe, D. M., Hildenbrand, D. L., and Lau, K. N., "Stability of supported metal and supported metal oxide combustion catalysts," *Catal Today*, vol. 47, pp. 5-17, 1999.
- [5] Hayek, K., Kramer, R., and Paal, Z., "Metal-support boundary sites in catalysis," *Appl Catal a-Gen*, vol. 162, pp. 1-15, 1997.
- [6] Brinker, C. J. and Scherer, G. W., "Sol-gel science-the physics and chemistry of sol-gel processing," *Academic press, inc. 1250 sixth avenue, San Diego, CA, 92101*, 1990.
- [7] Avci, A. K., Onsan, Z. I., and Trimm, D. L., "On-board hydrogen generation for fuel cell-powered vehicles: the use of methanol and propane," *Top Catal*, vol. 22, pp. 359-367, 2003.
- [8] Sinel'nikov, V. V., Tolkachev, N. N., Goryashchenko, S. S., Telegina, N. S., and Stakheev, A. Y., "Propane oxidation with chemically bound oxygen on Pt/TiO₂/Al₂O₃ and Pt/CeO₂/Al₂O₃ catalysts," *Kinet Catal+*, vol. 47, pp. 98-105, 2006.
- [9] Routray, K., Reddy, K. R. S. K., and Deo, G., "Oxidative dehydrogenation of propane on V₂O₅/Al₂O₃ and V₂O₅/TiO₂ catalysts: understanding the effect of support by parameter estimation," *Appl Catal a-Gen*, vol. 265, pp. 103-113, 2004.
- [10] Aartun, I., Gjervan, T., Venvik, H., Gorke, O., Pfeifer, P., Fathi, M., Holmen, A., and Schubert, K., "Catalytic conversion of propane to hydrogen in microstructured reactors," *Chemical Engineering Journal*, vol. 101, pp. 93-99, 2004.
- [11] Caglayan, B. S., Avci, A. K., Onsan, Z. I., and Aksoylu, A. E., "Production of hydrogen over bimetallic Pt-Ni/delta-Al₂O₃ - I. Indirect partial oxidation of propane," *Appl Catal a-Gen*, vol. 280, pp. 181-188, 2005.
- [12] Beretta, A. and Forzatti, P., "Partial oxidation of light paraffins to synthesis gas in short contact-time reactors," *Chemical Engineering Journal*, vol. 99, pp. 219-226, 2004.
- [13] Silberova, B., Venvik, H. J., and Holmen, A., "Production of hydrogen by short contact time partial oxidation and oxidative steam reforming of propane," *Catal Today*, vol. 99, pp. 69-76, 2005.
- [14] Solymosi, F., Tolmascov, P., and Kedves, K., "CO₂ reforming of propane over supported Rh," *J Catal*, vol. 216, pp. 377-385, 2003.
- [15] Marengo, S., Patrono, P., Comotti, P., Galli, G., Galli, P., Massucci, M. A., and Meloni, M. T., "Propane partial oxidation over M³⁺-substituted vanadyl phosphates dispersed on titania and silica," *Appl Catal a-Gen*, vol. 230, pp. 219-231, 2002.
- [16] Montoya, J. A., del Angel, P., and Viveros, T., "The effect of temperature on the structural and textural evolution of sol-gel Al₂O₃-TiO₂ mixed oxides," *J Mater Chem*, vol. 11, pp. 944-950, 2001.
- [17] Pettersson, L. J. and Westerholm, R., "State of the art of multi-fuel reformers for fuel cell vehicles: problem identification and research needs," *Int J Hydrogen Energ*, vol. 26, pp. 243-264, 2001.
- [18] Bacsá, R. R. and Kiwi, J., "Effect of rutile phase on the photocatalytic properties of nanocrystalline titania during the degradation of p-coumaric acid," *Appl Catal B-Environ*, vol. 16, pp. 19-29, 1998.
- [19] Subramanian, V., Ni, Z., Seebauer, E. G., and Masel, R. I., "Synthesis of High-Temperature Titania-Alumina Supports," *Ind Eng Chem Res*, vol. 45, pp. 3815-3820, 2006.
- [20] Hu, Y., Tsai, H. L., and Huang, C. L., "Effect of brookite phase on the anatase-rutile transition in titania nanoparticles," *J Eur Ceram Soc*, vol. 23, pp. 691-696, 2003.
- [21] Hu, Y., Tsai, H. L., and Huang, C. L., "Phase transformation of precipitated TiO₂ nanoparticles," *Mat Sci Eng a-Struct*, vol. 344, pp. 209-214, 2003.
- [22] Penn, R. L. and Banfield, J. F., "Oriented attachment and growth, twinning, polytypism, and formation of metastable phases: Insights from nanocrystalline TiO₂," *Am Mineral*, vol. 83, pp. 1077-1082, 1998.
- [23] Nair, K. and Kumar, P., "Growth of rutile crystallites during the initial stage of anatase-to-rutile transformation in pure titania and in titania-alumina nanocomposites," *Scripta Metallurgica et Materialia*, vol. 32, pp. 873-877, 1995.
- [24] Zhang, Y. H., Weidenkaff, A., and Reller, A., "Mesoporous structure and phase transition of nanocrystalline TiO₂," *Mater Lett*, vol. 54, pp. 375-381, 2002.
- [25] Yoo, Y. S., Kim, H., and Kim, D. Y., "Effect of SiO₂ and TiO₂ addition on the exaggerated grain growth of BaTiO₃," *J Eur Ceram Soc*, vol. 17, pp. 805-811, 1997.
- [26] Wang, C. B., Lin, H. K., and Ho, C. M., "Effects of the addition of titania on the thermal characterization of alumina-supported palladium," *J Mol Catal a-Chem*, vol. 180, pp. 285-291, 2002.
- [27] Kolb, G., Cominos, V., Hofmann, C., Pennemann, H., Schurer, J., Tiemann, D., Wichert, M., Zapf, R., Hessel, V., and Lowe, H., "Integrated microstructured fuel processors for fuel cell applications," *Chem Eng Res Des*, vol. 83, pp. 626-633, 2005.
- [28] Kolb, G., Zapf, R., Hessel, V., and Lowe, H., "Propane steam reforming in micro-channels - results from catalyst screening and optimisation," *Appl Catal a-Gen*, vol. 277, pp. 155-166, 2004.
- [29] Maillot, T., Barbier, J., Gelin, P., Praliaud, H., and Duprez, D., "Effects of pretreatments on the surface composition of alumina-supported Pd-Rh catalysts," *J Catal*, vol. 202, pp. 367-378, 2001.